Computational and Experimental Study of the Effect of Mass Transfer on Liquid-Jet Breakup

M. Situ* and J.A. Schetz†
Virginia Polytechnic Institute and State University, Blacksburg, Virginia

A computational method has been developed to predict the effect of mass transfer on liquid-jet breakup in coaxial, low-velocity gas streams. Two conditions, both with and without the effect of mass transfer on the jet breakup, are calculated and compared with experimental results and the classical linear theory. Methanol and water were used as the injectants. The numerical solution can predict the instantaneous shape of the jet surface and the breakup time. This solution is very close to the experimental results. The numerical solutions and the experimental results both indicate that the wave number of the maximum instability is about 6.9, higher than the 4.51 that was predicted by Rayleigh's linear theory. The experimental results and numerical solution show that the growth of the amplitude of the trough is faster than the growth of the amplitude of the crest, especially for a rapidly vaporizing jet. The numerical solutions show that, for the small rates of evaporation, the effect of the mass transfer on the interface has a stabilizing effect near the wave number for maximum instability. Inversely, it has a destabilizing effect far from the wave number for maximum instability. For rapid evaporation, the effect of the mass transfer always has a destabilizing effect and decreases the breakup time of the jet.

Nomenclature

a = jet radius
A = perturbation amplitude
A_0 = initial perturbation amplitude
c = adiabatic speed of sound
c_p = specific heat at constant pressure
D = jet diameter
D_{av} = diffusion coefficient
F = volume fraction of fluid in cell
$\bar{g}$ = vector of body acceleration
h = static enthalpy
k = thermal conductivity
l = length
L = latent heat
m = mass fraction
M = molecular weight
N = mole fraction
p = pressure
Pr = Prandtl number, $c_p\mu/k$
R = gas constant
$\bar{R}$ = radius of curvature
$\mathscr{R}$ = universal gas constant
Sc = Schmidt number, $\mu/\rho D_{av}$
t = time
T = temperature and nondimensional time
u = radial velocity component
v = axial velocity component
$\bar{v}$ = velocity vector
WN = wave number, λ/D
ρ = density
μ = viscosity
λ = wavelength
σ = coefficient of surface tension
τ = shear stress
$\dot{\omega}_v$ = vapor mass flux

Subscripts

a = air
B = breakup
F = fluid
g = gas
i = interface
j = component
s = saturation
v = vapor

Presented as Paper 83-1400 at the AIAA/SAE/ASME 19th Joint Propulsion Conference, Seattle, Wash., June 27-29, 1983; received Aug. 3, 1983; revision received Jan. 19, 1984.

*Visiting Scholar, Aerospace and Ocean Engineering Department.
†Professor and Head, Aerospace and Ocean Engineering Department. Associate Fellow AIAA.

Introduction

THE problem of liquid-jet breakup with heat and mass transfer in a gas flow is of interest and importance in the study of all airbreathing engines and liquid rocket engines, because the great majority of such engines at present do, and for some time probably will, derive their energy from liquid fuels. This general problem is also important in other technical areas, such as cooling sprays in turbines and localized cooling on re-entry bodies.

Jet breakup and droplet formation with the effects of heat and mass transfer are complicated phenomena, especially in the complex real flowfields in engines. The problem is complex even under idealized conditions. Joshi and Schetz[1,2] have offered an investigation of the linear stability of an evaporating liquid film of finite depth adjacent to a low-speed gas stream. A number of restrictive assumptions had to be invoked to permit relatively straightforward treatment. With the advent of the widespread use of large digital computers, one can hope to treat much less restrictive problems, although some simplifying assumptions are still necessary.

The instability of a laminar or inviscid liquid jet in a quiescent or coflowing gas medium has been investigated extensively in the past. The first analysis was published by Lord Rayleigh.[3] Rayleigh's theory showed that the disturbance amplitude A grows exponentially as

$$A = A_0 e^{qt} = A_0 e^{\bar{q}T} \tag{1}$$

where

$$q^2 = \left(\frac{\sigma}{\rho_F a^3}\right)\left[\frac{(1-k^2a^2)\cdot ika\cdot J_0'(ika)}{J_0(ika)}\right] = \left(\frac{\sigma}{\rho_F a^3}\right)F(ka) \tag{2}$$

$$T = t\left(\sigma/\rho_F a^3\right)^{\frac{1}{2}} \tag{3}$$

under certain conditions. $F(ka)$ is a function of $ka = 2\pi a/\lambda$ and $(\sigma/\rho_F a^3)^{\frac{1}{2}}$ is a coefficient of nondimensional time. Such a disturbance becomes amplified when the wavelength exceeds the jet circumference, an amplification that reaches a maximum when WN = 4.508. Rayleigh's linear theory neglected the influence of airflow, mass transfer, and viscosity. Other researchers have conducted further analyses and experiments.[4-9] For example, Weber [4] attempted to extend Rayleigh's analysis to include viscosity. The experiments in Refs. 6 and 9 have shown that the relation between linear instability and actual jet breakup is complex.

A number of phenomena occurring in nature and in modern engineering problems are essentially incompressible, and many of the earlier investigations were concerned with two incompressible fluids in parallel motion. Apart from the practical applications of incompressible flows, the fact that the incompressible problem is not yet completely understood provides motivation for the present work. Thus, a detailed examination of the incompressible case appears to be the logical first step. This case can help us to understand the mechanisms of the phenomena.

The present work is an attempt to develop a numerical calculation of the influences of mass and heat transfer on the nonlinear liquid-jet stability and breakup problem in essentially incompressible flow. All thermodynamic and transport properties in the flowfield (such as specific heat, viscosity, surface tension, saturated vapor pressure, thermal conductivity, and diffusion coefficient) are treated as variables expressed as functions of the temperature and the component mass fraction. A numerical code for solving the unsteady Navier-Stokes equations for flows with a free surface, developed by Los Alamos Scientific Laboratories,[10] was modified extensively by the addition of energy and diffusion equations for the gas stream and suitable boundary conditions on the interface in the gas flowfield for flows with mass transfer.

In order to have detailed data for use in verifying the adequacy of the numerical calculations, the present work also included an experimental investigation of the breakup and droplet formation of laminar liquid jets issuing into an airstream. The velocity of the airstream was varied. A nozzle with a 0.762 mm diam orifice was vibrated in the axial direction with an electromechanical vibrator. Water was used as a baseline case with negligible mass transfer for comparison. It is expensive and difficult to obtain a high-temperature airstream in a laboratory environment, so the effects of mass transfer were studied by using an injectant with a high vapor pressure at modest temperatures. Methanol was injected into room temperature air. The relevant properties of the two fluids are listed in Table 1. In order to keep the jets purely laminar, the Reynolds number of the jets were taken as 1000 for water and 600 for methanol.

It is pointed out that, as a first step, we will analyze the negligible mass transfer problem since this is much simpler. The numerical calculation result can be compared with our experimental results and the Rayleigh and Weber linear theories of the instability of the liquid jet. Next, the instability and breakup of the water jet in a high-temperature gas flowfield with heat and mass transfer was calculated in order to understand the basic phenomena when a jet is injected into a high-temperature gas stream. Finally, the instability and breakup of the methanol jet issuing into the airstream was calculated and compared with the present experimental results.

Analysis

For the heat and mass transfer problem, the liquid at the interface vaporizes and the vapor is entrained into the gas stream through convection and diffusion. The liquid and gas motion are assumed laminar. The temperature of the interface of the liquid has to be determined by the heat balance. Axisymmetric, nearly incompressible motion with heat and mass transfer on the interface is governed by the following equations:

Liquid,

$$\nabla \cdot \bar{v}_F = 0 \tag{4}$$

$$\frac{\partial \bar{v}_F}{\partial t} + \left(\bar{v}_F \cdot \nabla\right)\bar{v}_F = \bar{g} + \frac{\mu_F}{\rho_F}\nabla^2 \bar{v}_F - \frac{1}{\rho_F}\nabla p_F \tag{5}$$

$$\frac{\partial T_F}{\partial t} + \bar{v}_F \cdot \left(\nabla T_F\right) = \left(\frac{k_F}{\rho_F c_{pF}}\right)\nabla^2 T_F \tag{6}$$

Gas,

$$\frac{1}{\rho_g c^2}\frac{\partial p_g}{\partial t} + \nabla \cdot \bar{v}_g = 0 \tag{7}$$

$$\frac{\partial \bar{v}_g}{\partial t} + \left(\bar{v}_g \cdot \nabla\right)\bar{v}_g = \bar{g} + \frac{\mu_g}{\rho_g}\nabla^2 \bar{v}_g - \frac{1}{\rho_g}\nabla p_g \tag{8}$$

$$\frac{\mathrm{D}m_j}{\mathrm{D}t} = D_{\mathrm{av}}\nabla^2 m_j \tag{9}$$

$$\frac{\mathrm{D}T_g}{\mathrm{D}t} = \frac{k_g}{\rho_g c_{pg}}\nabla^2 T_g + \frac{1}{\rho_g c_{pg}}\nabla \cdot \left(\rho_g \sum_j D_{\mathrm{av}} h_j \nabla m_j\right) \tag{10}$$

In the continuity equation for the gas, it is desirable to allow for limited compressibility effects.[11] In the energy equation, the last term on the right-hand side describes the effect that energy transport is connected with diffusion even when no temperature gradients occur. This term can be neglected if Pr is approximately equal to Sc. In addition, the flow velocities are taken as sufficiently small, so that frictional heating can be neglected.

Boundary Conditions

In order to solve the above set of the governing equations, it is essential to specify appropriate boundary conditions. In the present numerical calculation, there are two kinds of boundary conditions, which should be considered separately.

Mesh Boundaries

When the differential method is adopted to solve the elliptic, partial differential equations numerically, it is necessary to generate a computing mesh throughout the flowfield. At the mesh boundaries, a variety of conditions may be set using the idea of fictitious cells surrounding the mesh. If this is a rigid free-slip wall, the normal velocity there must be zero and the

Table 1 Injectant parameters

	Water			Methanol		
T, °C	p_s, atm	$\sigma \cdot 10^3$, N/m	$\mu \cdot 10^3$, N · s/m^2	p_s, atm	$\sigma \cdot 10^3$, N/m	$\mu \cdot 10^3$, N · s/m^2
20	0.004	72.5	1.002	0.103	23.8	0.578
35	0.008	70.1	0.734	0.265	22.2	0.475
50	0.012	67.8	0.544	0.527	21.0	0.393

tangential velocity should have no normal gradient. If it is a no-slip rigid wall, then the tangential velocity component at the wall should also be zero.

Interface Boundaries

The interface boundary is still considered to be a free boundary. It is seen that the discontinuity in the normal stresses across the interface must be balanced by surface tension. Thus,

$$p_g - p_F = \sigma/\bar{R} \tag{11}$$

The interface boundary condition for normal stress is automatically satisfied by the implicit pressure calculation and the specification of velocities immediately outside the surface. The balance of shear stresses at the interface is $\tau_g = \tau_F$ on the interface. The velocities on the neighboring empty cell of the surface cell are assumed to satisfy the balance of shear stresses at the interface.

In addition, the heat and mass balance at the interface must be set:

1) No temperature jump at the interface

$$T_g(x, y, t) = T_F(x, y, t) \text{ on the interface} \tag{12a}$$

2) Energy balance at the interface

$$k_F \nabla T_F - k_g \nabla T_g = \dot{\omega}_v L \tag{12b}$$

3) Injection velocity on the interface. If provisions are made that no air passes through the interface, the injection velocity on the interface[12] is

$$u_i = -\frac{D_{av}}{(1 - m_v)} \left(\frac{\partial m_v}{\partial x} \right)_i \tag{13}$$

The vapor mass flux $\dot{\omega}_v$ is determined by thermodynamic conditions. The saturation condition fixes the partial pressure of the vapor at the interface temperature. In turn, the partial pressure of the vapor determines the interface vapor mass fraction m_v. The phase equilibrium is expressed by the Clausius-Clayperon equation as

$$p_s = Be^{-L/RT_s} \tag{14}$$

where B is constant determined by some reference condition. For many substances, we may write $L = a + bT$, where a and b are constants. Also, p_s is the partial pressure of the vapor at temperature T_s. Thus, $p_s = (N_v/N_g)p_g$, so that the vapor partial pressure

$$p_v = m_v \left(\frac{M_g}{M_v} \right) p_g \tag{15}$$

and

$$m_v = \frac{p_v}{p_g} \left(\frac{M_v}{M_g} \right)$$

Thermodynamic and Transport Properties

The air and vapor are regarded as ideal gases. The viscosity and the surface tension of the liquid can be expressed as a function of temperature. These values can be obtained from Refs. 13 and 14. The viscosity of the gas was determined by the mixture equation of Ref. 15. The thermal conductivity can be expressed by the Prandtl number $Pr = \mu c_p/k$. The diffusion coefficient D_{av} can be calculated by a Schmidt number,

$$D_{av} = \mu/\rho Sc$$

Free Surface

The free surface location is computed from the volume fraction of fluid contained in each cell of the mesh. The fractional volume of the fluid scheme for tracking interface boundaries is

$$\frac{\partial F}{\partial t} + \frac{\partial (xFU_F)}{x \partial x} + \frac{\partial (FV_F)}{\partial y} = 0 \tag{16}$$

Computational Grid

The computational grid used was 20×20 cells. Liquid occupied about 40% of the total cells; gas occupied the other part of the total. The initial relative maximum perturbation amplitude/jet diameter was 0.0005. One hour of CPU execution time on an IBM 3032 computer was required to calculate the jet breakup for small rates of evaporation and low gas stream velocity. More than 1 h was required to calculate the jet breakup for higher rates of evaporation and high gas stream velocity.

Experimental Apparatus and Methods

Test Facility

A schematic of the test facility is shown in Fig. 1. An ejector was used to produce the airflow in the test section. In order to avoid the effects of the noise of the ejector, a rubber tube was used to connect the airflow conduit. The test section is a circular plastic tube with a diameter of 15 cm and a length of 100 cm.

Injection System

The liquid was delivered from a storage tank pressurized with nitrogen. The mass flow rate was measured with a Rotameter. Adjustments of the flow rate were made with a needle valve. A nozzle diameter of 0.762 mm was used.

Disturbance System

The basic unit was an electrical shaker driven by an audio-oscillator and a power amplifier. This could cover a frequency range of 10-8000 cycles/s. Figure 2 shows the setup.

Flash Shadowgraphs

To obtain shadowgraphs, a Nanopulser flash was used to backlight the liquid jet. The flash duration was approximately

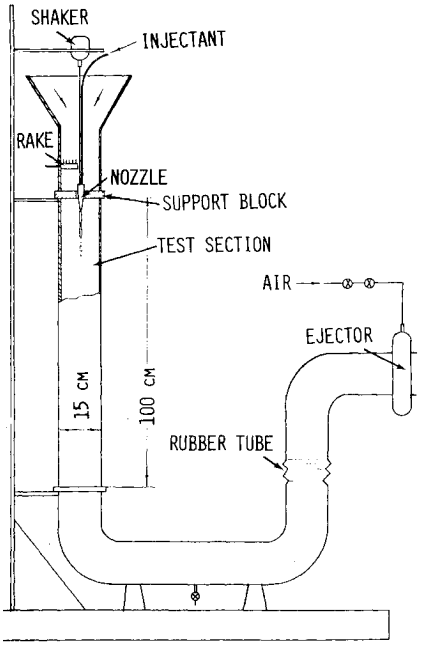

Fig. 1 Test facility.

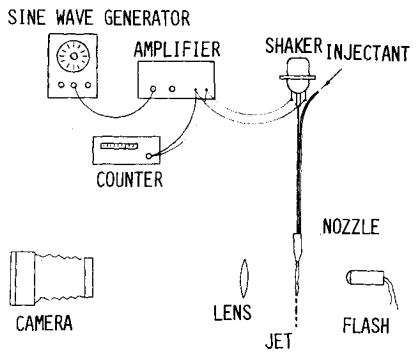

Fig. 2 Optical system and initial perturbation system.

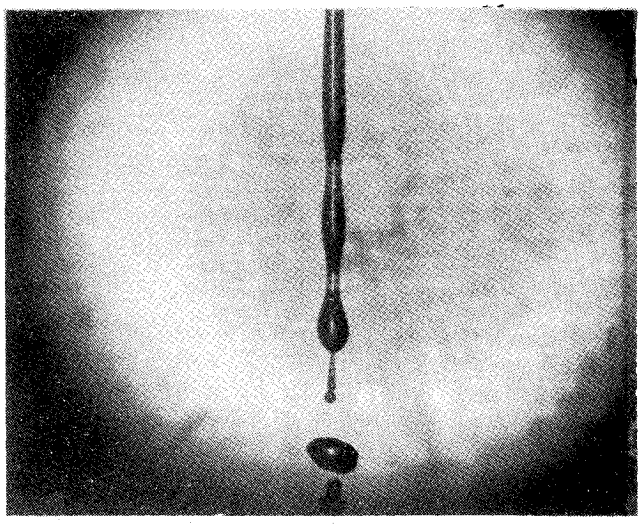

Fig. 3 Water jet breakup in air velocity of 2.0 m/s (WN = 5.50).

10^{-8} s. A lens was used to focus the image on a Polaroid 4 × 5 Land film. Type 57 Polaroid film was used, because a high sensitivity was required due to the extremely short exposure time.

Experimental Procedure

The desired jet flow rate was set using the needle valves and always kept stable, after which the desired velocity of the airstream was set. The oscillator had also been set to the predetermined frequency. In order to increase its evaporation, the temperature of the methanol was kept to 29°C, while the temperature of airstream was kept to 26°C. The jet velocity was varied between 0.5-1.5 m/s.

The instantaneous perturbation amplitudes of the various cycles in the photographs were obtained by using a precision optical comparator. The perturbation amplitudes of the trough and the crest were measured to 0.02 mm accuracy and compared with the numerical results.

The nondimensional breakup time T_B is related to the distance from the nozzle to breakup l_B by the relation

$$T_B = \frac{l_B}{v_F}\left(\frac{\sigma}{\rho_F D^3}\right)^{\frac{1}{2}} \tag{17}$$

v_F can be calculated from wavelength λ, which was obtained from the experiments. A series of characteristic jet forms can be seen on all of the photographs. A typical example is shown in Fig. 3. The shape of the jet is subject to small background disturbances, such as imperfect roundness of the orifice, vibrations of the whole apparatus, and particles of dust or bubbles in the jet.

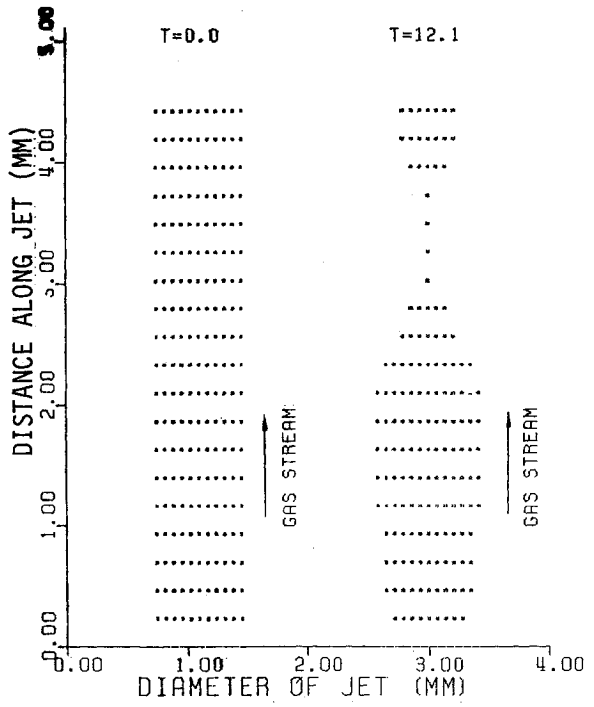

Fig. 4 Fluid configuration calculated for water jet (WN = 5.50, v_a = 2.0 m/s).

Results and Discussion

Six cases are considered in detail and the numerical results compared with the experimental results and the linear theory. The first three cases do not consider the effects of the heat and mass transfer, but the next three do consider these effects on the interface. In the first case, the instantaneous nondimensional perturbation amplitude was compared with experiment for a water jet with a wave number of 5.50. The instantaneous shape of the jet was drawn by computer and compared with the surface of the jet from experiment. Next was the nondimensional breakup time of the jet for different wave numbers, and the predictions were compared with the experimental results. In the third case, the breakup time of the jet for different velocities of the airstream was obtained from experiments, and the results were compared with numerical predictions at the lower air velocities. In the fourth, the perturbation amplitudes of the jet both with and without heat and mass transfer for two wave numbers were calculated and compared. The fifth case showed the effects of four different air temperatures. The last case considered the methanol jet, and predictions and experiment were compared for a wave number of 5.43.

Figure 4 shows the predicted instantaneous jet shape just before the jet breaks. The formation of a small cylinder can be seen. When the end of the cylinder breaks, one or two small drops (i.e., satellite droplets) are formed because of surface tension. This behavior is similar to that observed in the experiment (see Fig. 3). The shapes of the jet surface, both from the numerical results and from experiment at a nondimensional time of 11.10 are presented in Fig. 5. The numerical prediction of the surface shape is very close to the surface shape from the experiments.

In Fig. 6, the numerical predictions are compared with the experimental results and Rayleigh's theory in terms of nondimensional amplitude of the surface vs nondimensional time. As can be seen from the graph, the growth of the disturbance for a trough or for a crest is not simply exponential. The experiments of Ref. 6 had also indicated this nonlinear characteristic. In a moving stream, the jet perturbation amplitude of the trough is more than the perturbation amplitude of the crest because of the nonlinear effect of the airstream and the

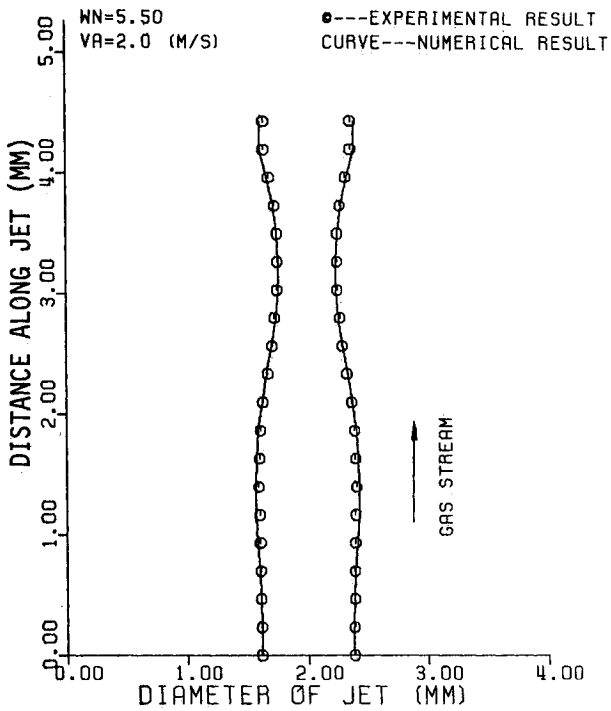

Fig. 5 Numerical prediction of surface shape compared with surface shape from experiment for water jet at $T = 11.10$.

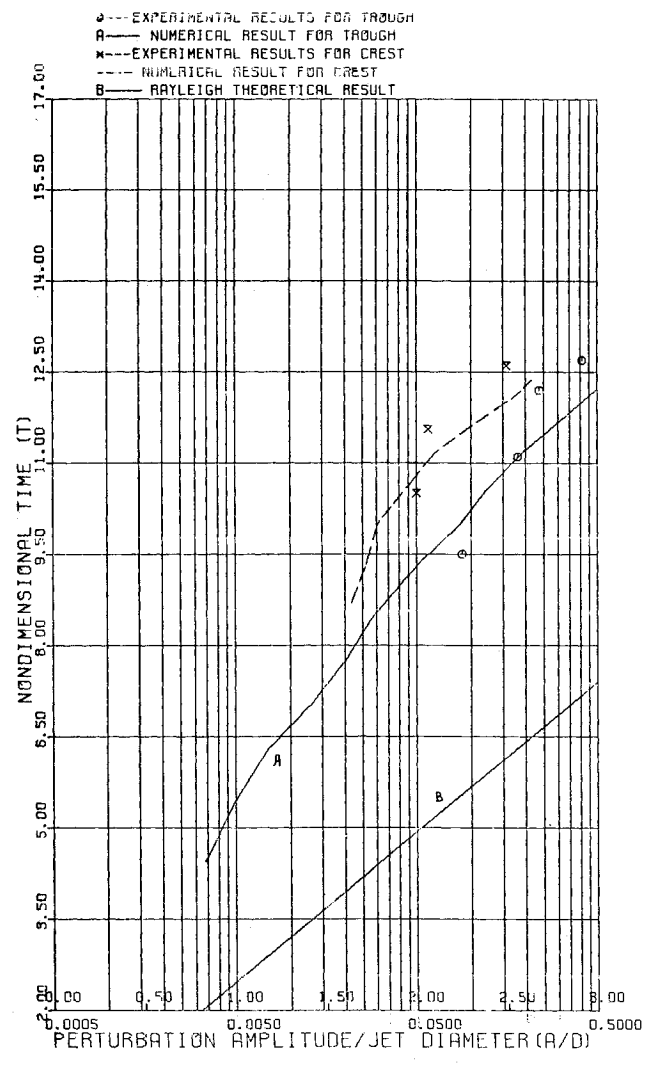

Fig. 6 Perturbation amplitude for water jet plotted against nondimensional time (WN = 5.50, $v_a = 2.0$ m/s).

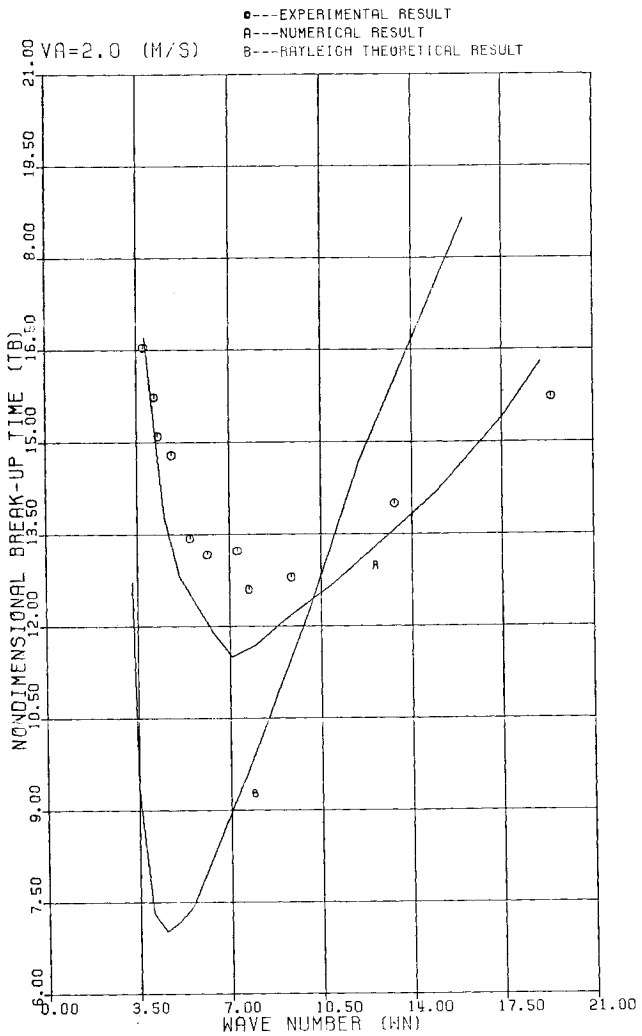

Fig. 7 Nondimensional breakup time of water jet plotted against wave number (WN).

viscosity of the liquid. This is predicted by the numerical solution. Rayleigh's theory cannot cover this problem.

Figure 7 shows the breakup time against the wave number ($WN = \lambda/D$). Curve B is Rayleigh's linear result indicating that the jet breakup is very fast and that the variation around the wave number of maximum instability (4.51) is very steep. Curve A is the current numerical nonlinear result. Curve A indicates that the jet breakup time is longer than Rayleigh's prediction, the wave number of the maximum instability is about 6.9, and the variation is not so steep around the wave number for maximum instability because of the effects of the viscosity and the gas stream. These curves are compared with the experimental results. It is obvious that the current numerical, nonlinear result is much closer to the experimental results. The wave number of the maximum instability from experimental results is about 7.5. The numerical solutions showed that, when the perturbation amplitude is very small, the wave number of maximum instability is 4.8, which is close to that of Rayleigh's linear result of 4.51. Rayleigh's theory is good only for infinitesimal amplitudes neglecting the effect of the liquid viscosity and the airstream.

Figure 8 shows the jet breakup and droplet formation with a high-speed airstream for a wave number of 5.50. At the lower velocities, the airstream does not appreciably affect the shape and breakup of the jet. The numerical solution also predicted these phenomena. This behavior can be explained by the fact that the aerodynamic force on the interface due to the air velocity is very small at the lowest velocities. The only

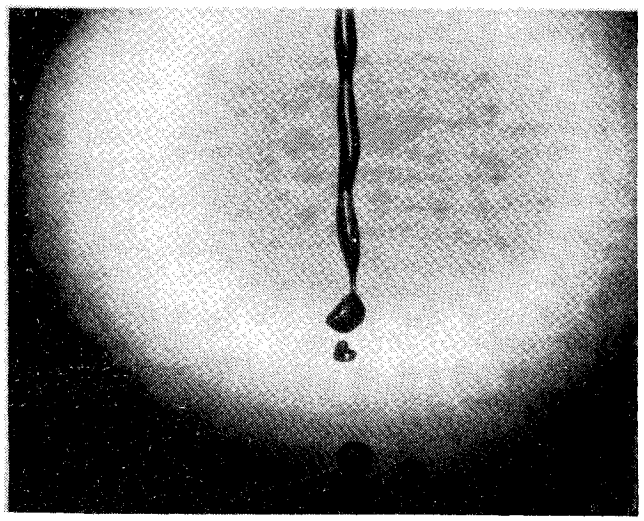

Fig. 8 Water jet breakup in air velocity of 35.0 m/s (WN = 5.50).

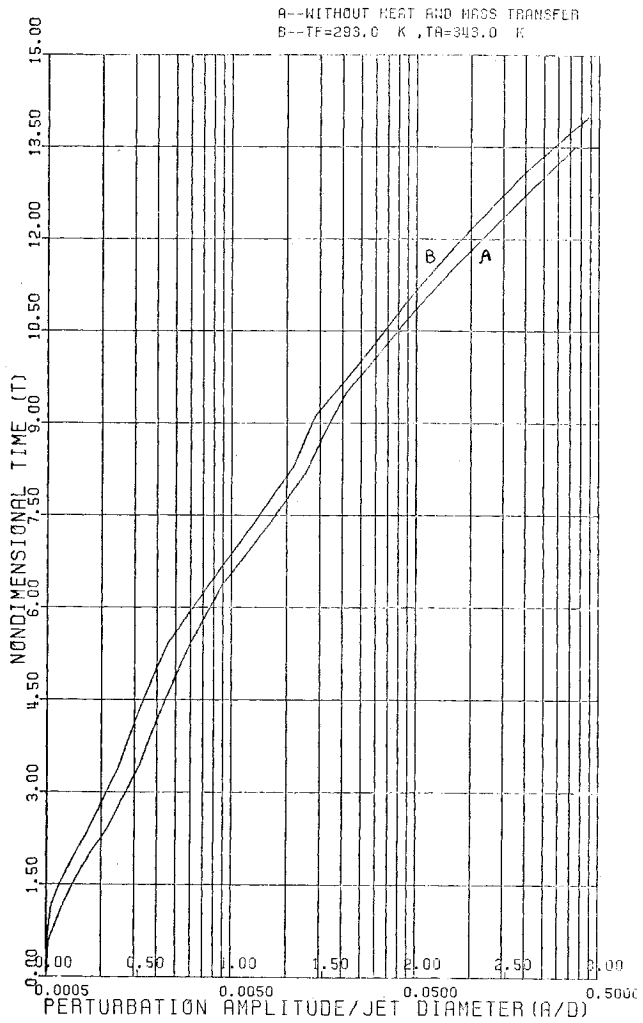

Fig. 9 Variation of perturbation amplitude with nondimensional time with the effect of mass transfer (v_a = 2.0 m/s, WN = 4.51).

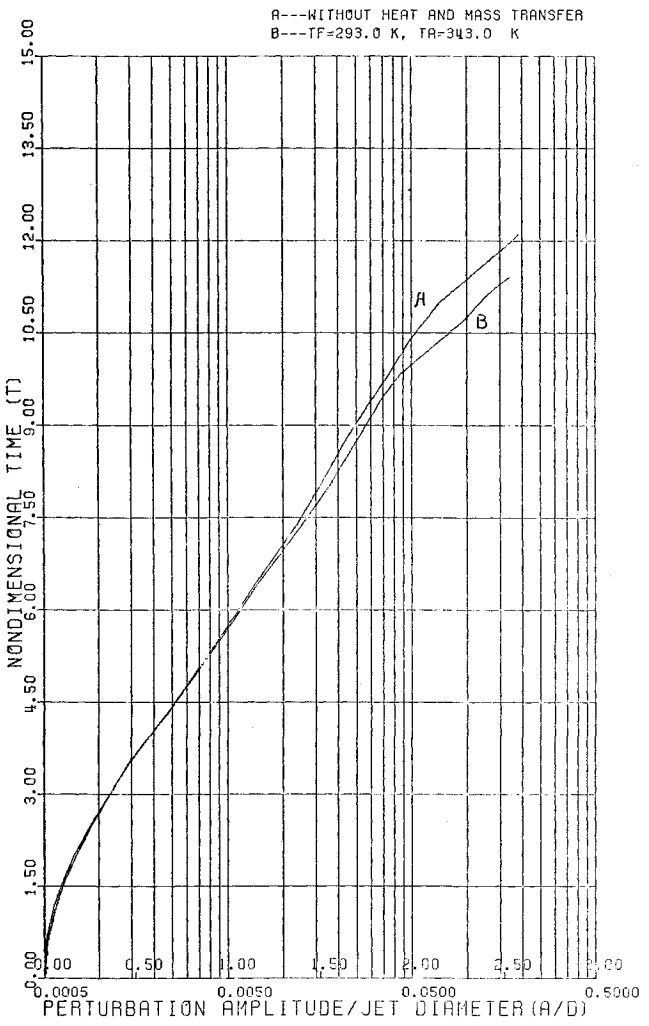

Fig. 10 Perturbation amplitude plotted against nondimensional time with the effect of mass transfer (v_a = 2.0 m/s, WN = 11.0).

disturbing force then acting on the jet is the surface tension. At an airflow velocity of about 5.0 m/s, the jet begins to develop a nonaxisymmetric shape. With further increases in the velocity of the airstream, the breakup time decreases.

The predicted perturbation amplification curves for liquid jets, with and without the effects of mass transfer, for two different wave numbers are given in Figs. 9 and 10. For small rates of evaporation, the surface tension and viscosity on the jet surface did not vary because the temperature of the jet surface is similar to that without the effect of mass transfer. Thus, it is observed that the effect of the heat and mass transfer on the interface indicates stabilization of a liquid jet at a wave number of 4.51. When the wave number is 11.0, the effect of the mass transfer on the interface represents a destabilization of the jet. These results are similar to those from the linear theory of Ref. 1. Figure 11 shows that, as the air temperature is increased, the effect of heat and mass transfer is to destabilize the interface. At the beginning of the perturbation, the jet interface will be contracted because of the rapid mass transfer on the interface. Then, the flowfield with heat and mass transfer tends to a balanced condition and the mass transfer rate from the interface decreases. After that time, only the effects of the hydrodynamic instability are important.

Figure 12 shows a typical photograph of the breakup of methanol jets in an airflow of 2 m/s. The breakup of the methanol jets is qualitatively similar to the breakup of water jets. The formation of the small cylinder is again seen.

Figure 13 shows the instantaneous jet shape from the numerical solution plotted by computer. At the jet's breakup, when the nondimensional time is 9.03, the jet shape from the numerical solution is very similar to that at breakup from the experiments. The shapes of the methanol jet surface, from both numerical prediction and experiment at $T = 8.234$ are presented in Fig. 14. Basically, they are identical, but the jet shape from experiment is slightly thinner than predicted by

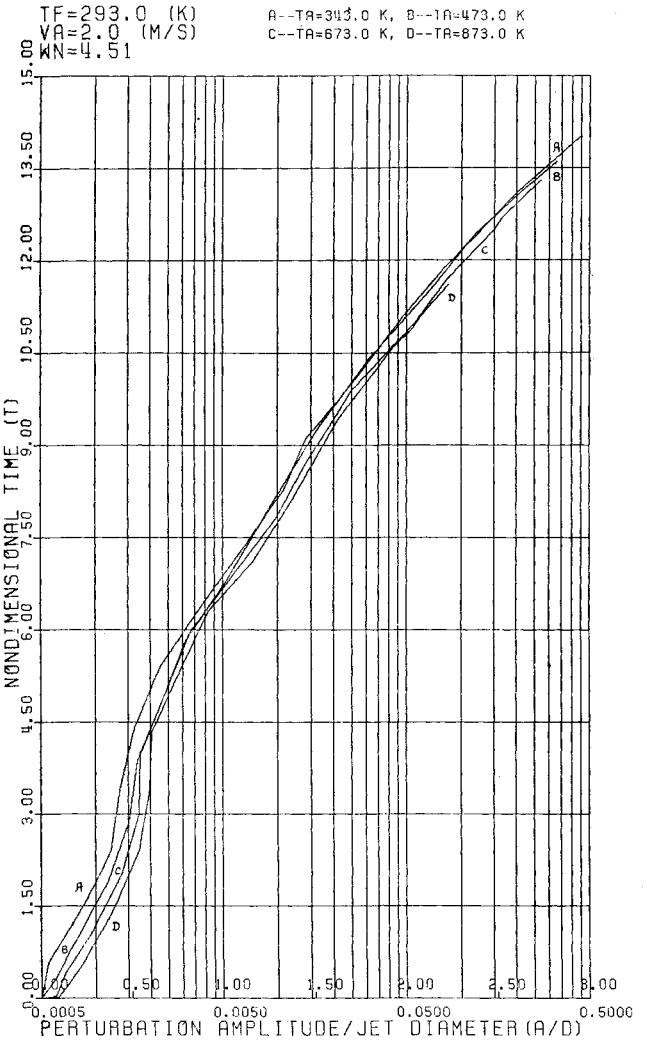

Fig. 11 Perturbation amplitude plotted against nondimensional time for different air temperatures.

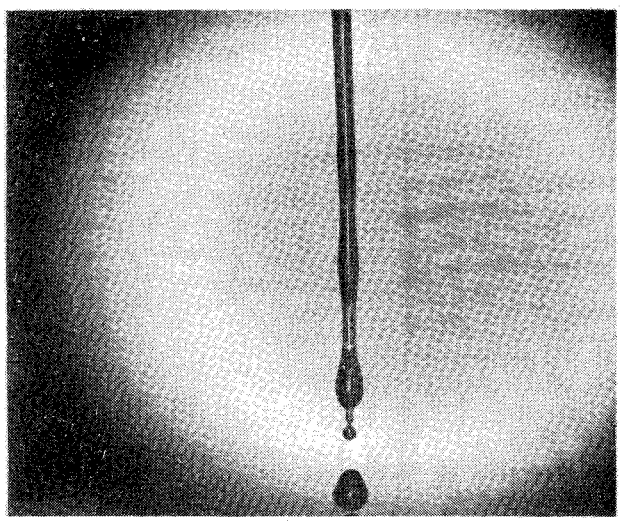

Fig. 12 Breakup of methanol jet in air velocity of 2.0 m/s (WN = 5.43, T_F = 302 K, T_a = 299 K).

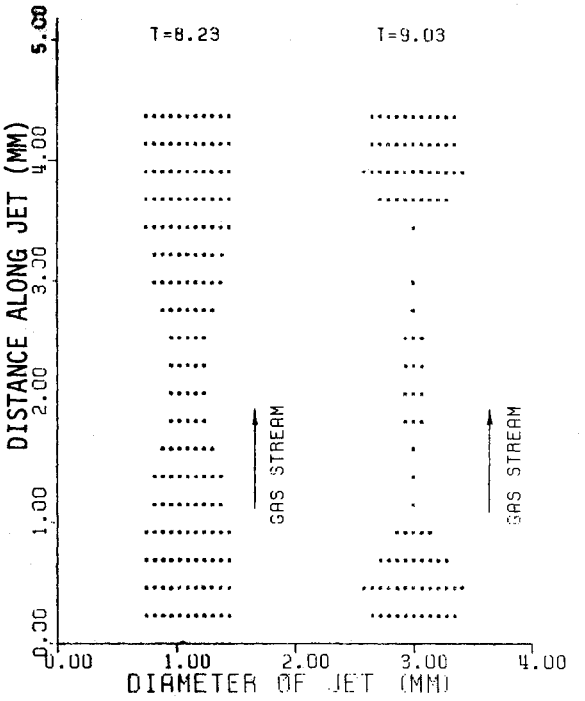

Fig. 13 Fluid configuration calculated for methanol jet (v_a = 2.0 m/s, WN = 5.43, T_F = 302 K, T_a = 299 K).

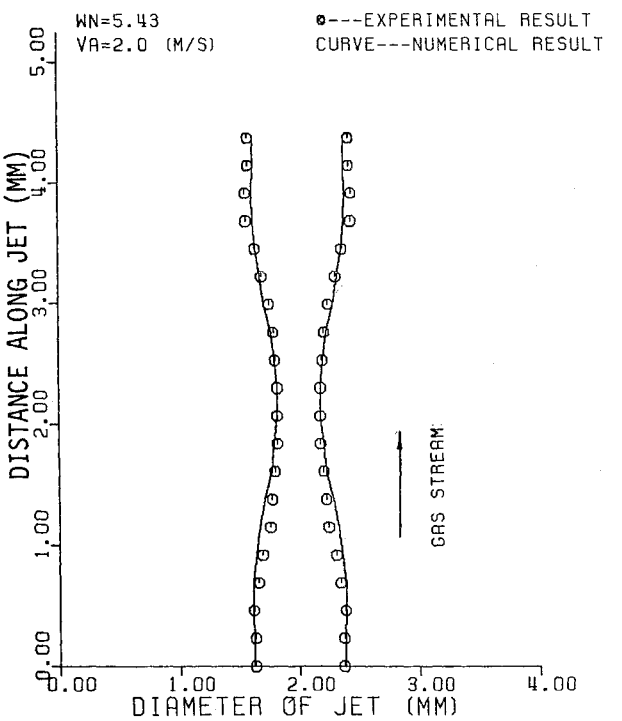

Fig. 14 Numerical prediction of a methanol jet surface shape compared with surface shape from experiment at T = 8.234, T_F = 302 K, T_a = 299 K.

the numerical result. The relation of the nondimensional perturbation amplitude against the nondimensional time is shown in Fig. 15. It is obvious that before the breakup of the methanol jet, the nondimensional perturbation amplitude of the crest first decreased and was less than the initial value (0.0005). The experimental and numerical results both showed this phenomenon, but the experimental effect was less than found by numerical solutions. Taken together, these results

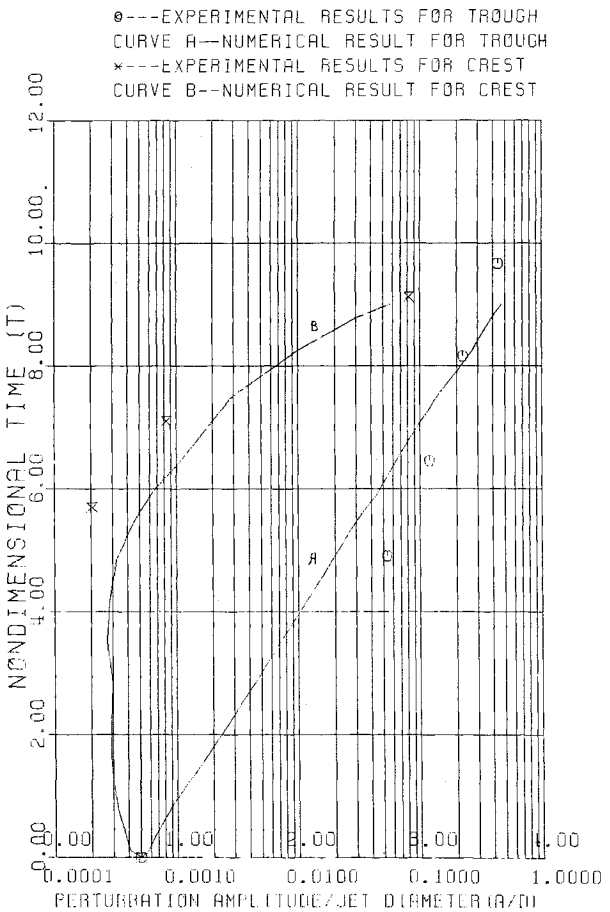

Fig. 15 Perturbation amplitude of a methanol jet plotted against nondimensional time (v_a = 2.0 m/s, WN = 5.43, T_F = 302 K, T_a = 299 K).

convincingly show that the numerical procedure developed is capable of excellent predictions for this complex flow problem.

Conclusions

The main purpose of this study was to investigate the effects of mass transfer on the instability and breakup of a liquid jet. In the regime of a low-speed coaxial gas stream, a small axisymmetric perturbation that is spatially sinusoidal along the length of the column grows and thus causes breakup. With increasing velocity of the gas stream, the shape of the jet changed to the "snake" and "sausage" modes. The helical phase also becomes more exaggerated. The numerical solution can predict the jet shape and breakup time in the lower air velocity regime. The numerical solution and the experimental results both indicate that the wave number of the maximum instability is about 6.9. When the instantaneous perturbation amplitude of the jet is very small, the wave number of maximum instability is close to 4.51, which was predicted by Rayleigh's theory.

The experimental results also showed that the perturbation amplitude of the crest and the perturbation amplitude of the trough were different. The growth of the amplitude of the trough is faster than the growth of the crest amplitude. This is identical with the prediction of the numerical solution, which also indicated the instantaneous growth of the perturbation amplitude has a nonlinear character.

For small heat and mass transfer rates, it was found that the interface evaporation and the variation of the interface temperature had a destabilizing effect when the wave number was large or small. The numerical results indicated that, when the temperature and vaporization in the gas stream tended to balance, hydrodynamic instability was still the most important factor.

Most importantly, comparison of numerical predictions and experimental results over a wide range of conditions shows that the nonlinear numerical solution method is capable of accurate predictions of perturbation growth and jet breakup, including the important and complex effects of surface mass transfer.

Acknowledgment

This work was supported in part by the Air Force Office of Scientific Research with Dr. J. Tishkoff as Technical Monitor.

References

[1]Joshi, P.B. and Schetz, J.A., "Hydrodynamic Stability of Liquid Films Adjacent to Incompressible Gas Streams Including Effects of Interface Mass Transfer," VPI-Aero-058, AFOSR-74-2584, 1976.

[2]Joshi, P.B. and Schetz, J.A., "Stability of a Liquid Gas Interface with Phase Change," ASME Paper 81-WA/FE-22, 1982.

[3]Rayleigh, L., "On the Instability of Jets," *Proceedings of the London Mathematical Society*, Vol. 10, 1878.

[4]Weber, C., "Zum Zerfall eines Flüssigkeitsstrahles," *Zeitschrift fuer Angewandte Mathematik und Mechanik*, Vol. 11, No. 3, 1931.

[5]Chandrasekhar, S., *Hydrodynamic and Hydromagnetic Stability*, 1961, Clarendon Press, Oxford, England, 1961; republished by Dover Publications, New York, 1981.

[6]Crane, L., Birch, S., and McCormack, P.D., "The Effect of Mechanical Vibration on the Break-up of a Cylindrical Water Jet in Air," *British Journal of Applied Physics*, Vol. 15, 1964, p. 743.

[7]Shokoohi, F., "Numerical Investigation of the Disintegration of Liquid Jets," Ph.D. Dissertation, Columbia University, New York, 1976.

[8]Bogy, D.B., "Drop Formation in a Circular Liquid Jet," *Annual Review of Fluid Mechanics*, Vol. 11, 1979, pp. 207-228.

[9]Goedde, E.F. and Yuen, M.C., "Experiments on Liquid Jet Instability," *Journal of Fluid Mechanics*, Vol. 40, 1970, pp. 495-511.

[10]Nichols, B.D., Hirt, C.W., and Hotchkiss, R.S., "SOLA-VOF: A Solution Algorithm for Transient Fluid Flow with Multiple Free Boundaries," University of California, Los Angeles, Rept. LA-8355, 1980.

[11]Hirt, C.W. and Nichols, B.D., "Adding Limited Compressibility to Incompressible Hydrocodes," *Journal of Computational Physics*, Vol. 34, 1980, p. 34.

[12]Eckert, E.R.G. and Drake, R.M. Jr., *Heat and Mass Transfer*, McGraw-Hill Book Co., New York, 1959.

[13]Vargaftik, N.B., *Tables on the Thermophysical Properties of Liquids and Gases*, John Wiley & Sons, New York, 1975.

[14]Weast, R.C., *CRC Handbook of Chemistry and Physics*, 62nd Ed., CRC Press, Inc. Boca Raton, Fla., 1981-1982.

[15]Buddenberg, J.W. and Wilke, C.R., "Calculation of Gas Mixture Viscosities," *Industrial and Engineering Chemistry*, Vol. 41, 1949, p. 1345-1347.